JOURNAL OF MATERIALS SCIENCE 21 (1986) 4029–4034

Amorphous phase formation and stability in W–Ti–Si metallization materials

R. K. BALL, W. G. FREEMAN, A. J. TAYLOR, A. G. TODD
GEC Research Ltd., Hirst Research Centre, East Lane, Wembley, Middlesex HA9 7PP, UK

The range of composition over which co-sputtered alloys in the W–Ti–Si system are deposited in the amorphous state has been determined. Alloys are found to be crystalline only if they contain less than ~10% Si and this is associated with the presence of terminal solid solutions in the respective binary phase diagrams. The stability of W–Si amorphous alloys was examined using differential scanning calorimetry and X-ray diffraction. The most stable glasses exist in the range 10 to 30% Si and about the WSi_2 composition. There is some correlation between increasing stability and increasing activation energy for crystallization.

1. Introduction
Considerable research effort [1, 2] has been devoted to determining the range of formation and stability of liquid quenched, amorphous alloys, such that there is now a substantial body of data relating to binary, ternary and more complex alloys. Vapour phase deposited amorphous alloys have received less attention, particularly with regard to systems more complex than binary. We have determined the glass forming range of the W–Ti–Si system and the stability of certain binary and ternary compositions when the alloys are deposited by co-sputtering.

This system was chosen because its binary and ternary alloys are increasingly employed as gate metallizations [3, 4], contacts [5, 6] and diffusion barrier layers [7, 8] in semiconductor devices. The initial condition of such films varies from coarsely polycrystalline to amorphous, and depends strongly on composition and deposition parameters. The initial condition of the film can exert a strong influence on its subsequent behaviour. An example is the concept of employing diffusion barriers in the amorphous state thereby eliminating grain boundary diffusion. Several laboratories [9, 10], including the Hirst Research Centre [11], have shown that, at least at temperatures $< 500^\circ$ C, amorphous deposits are superior to their polycrystalline counterparts.

Determination of the initial state and subsequent thermal stability of films is therefore of practical importance and the aim of this work was to provide such information for the W–Ti–Si system.

2. Experimental procedures
The alloys were deposited in the form of ~200 nm thick layers in a Microvac 650 sputtering unit (Ion Tech Ltd, Teddington, UK) which incorporates three independently controlled, water-cooled d.c. magnetrons in a triangular array, sputtering upward onto inverted substrates. By varying the position of the substrates relative to the "focus" of the magnetron cluster, a wide range (~30 at % variation in any component) of alloy compositions can be obtained in a single run. A corollary of this is that some compositional variation can occur across a given substrate and the compositions quoted below are mean values with an estimated spread of ± 1.5 at % of each element. For all deposition runs, elemental targets (99.9 at % Ti; 99.95 at % W; 99.999 at % Si) were employed. Sputtering was carried out at a pressure of 1.5×10^{-3} torr using argon supplied by a BOC Rare Gas Purifier-4. Substrate temperatures were typically 50 to 60° C.

The structural nature of deposited films was determined using a standard glancing angle X-ray diffraction (XRD) technique while composition was determined by X-ray fluorescence analysis using copper as the substrate material. In most cases the crystallization temperature of the experimental alloys was determined using a Perkin–Elmer DSC-4 differential scanning calorimeter. Films for DSC analysis were mostly deposited on aluminium foil, since this could be folded to provide a sample with adequate mass ($\leqslant$ 1 mg) of alloy, but comparisons with films on copper foil and films stripped off the substrate were also made. A standard heating rate of 40° C min^{-1} was employed with the sample protected by a dynamic atmosphere of argon. The upper limit of the equipment is 600° C and a limited number of determinations above this temperature were carried out using room temperature XRD of films on glass substrates previously sealed under vacuum (better than 10^{-6} torr) in glass ampoules and furnace heated at 12° C min^{-1} to the required temperature.

To determine compatibility with device technology, the crystallization behaviour of W–Si was determined by XRD of films deposited on silicon and thermal oxide (100 nm) on silicon previously heat-treated isothermally under a dynamic atmosphere of nitrogen.

3. Results
3.1. Glass forming range
Films were taken to be amorphous if X-ray diffraction showed a diffuse halo characteristic of glass and no discernible diffraction lines. Each of the three binary

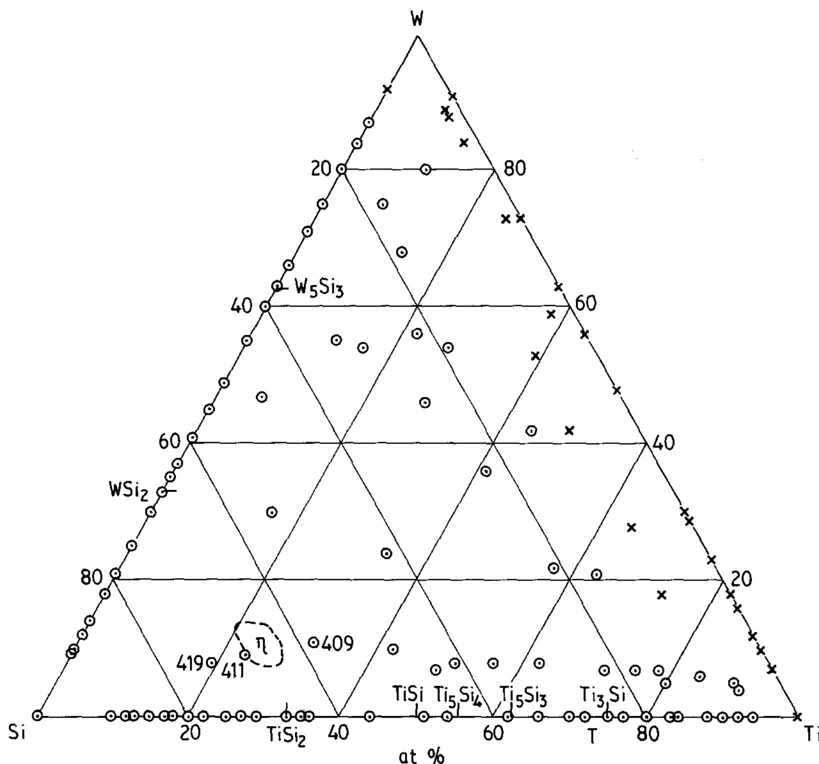

Figure 1 W–Ti–Si ternary diagram indicating the amorphous or crystalline nature of as-deposited alloys. Included are the equilibrium phases in the system together with some crystallization temperatures of glasses having compositions near the η phase. ×, crystalline; ⊙, amorphous.

systems W–Si, Ti–Si and Ti–W were examined in sufficient detail to define the limits of the glass forming range (GFR) to within a few atomic per cent. This is illustrated in Fig. 1, which shows that Ti–W behaves very differently from the two other binaries in that no completely amorphous phase is detected at any composition. In contrast the W–Si and Ti–Si systems show amorphous ranges extending from ~10 at % Si and ~6 at % Si, respectively, to 100 at % Si.

To determine the glass forming range in the ternary system, some 40 ternary samples were produced, analysed and subjected to XRD examination. Fig. 1 shows that crystalline as-deposited films were generally confined to compositions containing less than ~10 at % Si.

3.2. Stability of amorphous alloys

The temperatures corresponding to the onset of crystallization of a large number of amorphous binary and a few ternary alloys were determined using differential scanning calorimetry with a heating rate of 40° C min^{-1}. As a preliminary exercise, XRD was employed to confirm that the observed exothermic event corresponded to crystallization (Fig. 2). No reaction between the aluminium foil substrate and W–Si films was observed, but with Ti–Si a clear interaction was observed above ~35 at % Ti and an unambiguous determination of crystallization could not be achieved at titanium concentrations greater than this. It has been observed [12] that, unlike many other transition elements, titanium is capable of breaking through an Al_2O_3 surface layer to react with aluminium at ~450° C.

To assess the possible effect of the aluminium foil on the crystallization temperature, the latter was also determined for some compositions on copper foil and on deposits sufficiently poorly adherent to the aluminium foil to allow them to be stripped off. The

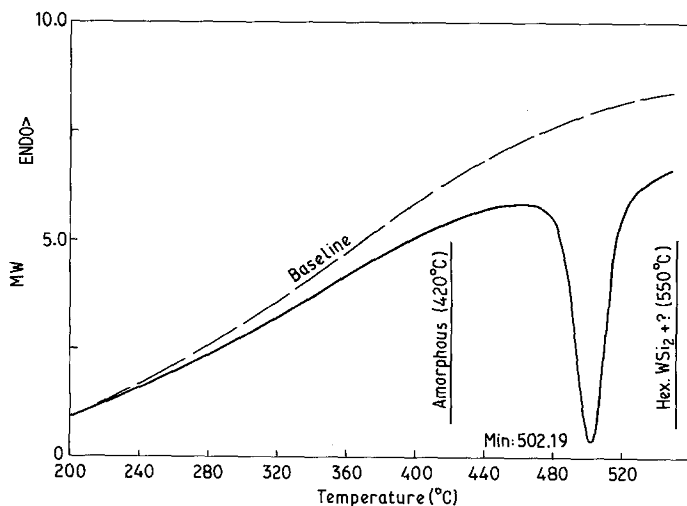

Figure 2 Differential scanning calorimeter trace of an amorphous $W_{54}Si_{46}$ thin film on an aluminium substrate. Included are the results of phase determination by glancing angle X-ray diffraction either side of the exothermic peak. Scan rate, 40.00 deg min^{-1}. Peak from 441.1 to 547.8. Onset, 493.65.

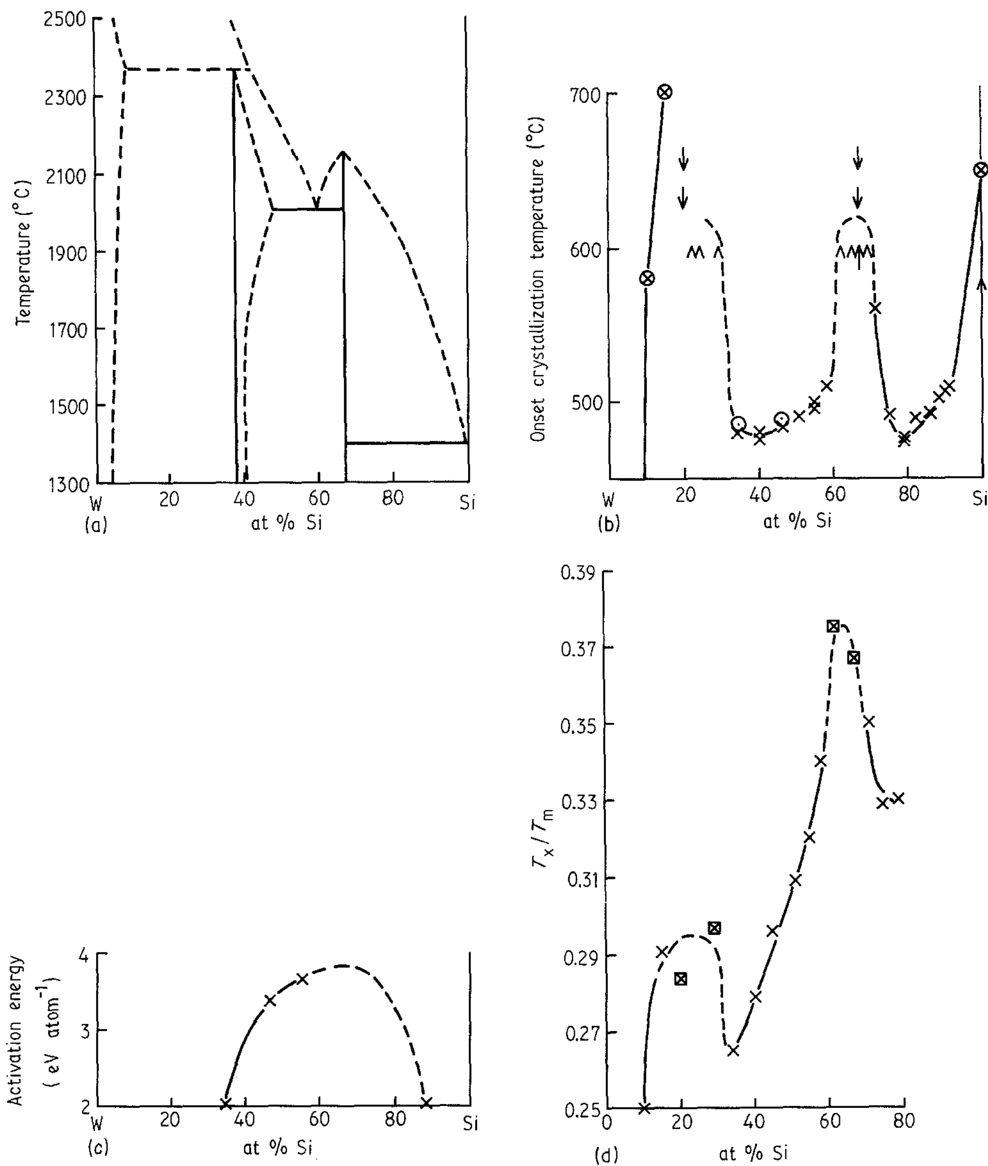

Figure 3 (a) Equilibrium phase diagram for W–Si. (b) Crystallization temperatures for W–Si amorphous alloys: ×, DSC, 40° C min^{-1}, onset temperature, Al substrate. ⊙, DSC, 40° C min^{-1}, onset temperature, Cu or no substrate. ⊗, reported data [27, 28]. ∧, DSC, 40° C min^{-1}, Al or no substrate. Crystallization does not occur below this temperature. ↑/↓, Furnace anneal (12° C min^{-1}) plus XRD. Glass crystallizes above/below this temperature. (c) Activation energy for crystallization against composition. (d) Reduced glass crystallization temperature for W–Si amorphous alloys. ⊠, estimated.

experiments show that the crystallization of W–Si is insensitive to the nature of the substrates chosen. However, with Ti–Si there is a relatively small but clear difference in crystallization behaviour between films on aluminium foil and those stripped off, probably due to a limited interaction between film and substrate.

The complete data regarding the onset of crystallization for W–Si alloys on aluminium and copper substrates and with no substrate (all determined by DSC at 40° C min^{-1}) together with data from furnace annealed films (12° C min^{-1}) on glass whose substrate condition was ascertained by XRD, are recorded in Fig. 3, together with the equilibrium phase diagram for this system. It can be seen that the crystallization temperature varies widely across the system with at least three maxima across the amorphous range. For several compositions the temperature corresponding to the crystallization peak in the DSC trace was determined as a function of heating rate (10 to 80° C min^{-1}). Using the Kissinger equation [13], which Ozawa [14] has shown is applicable to DSC measurements, this information may be displayed on the type of plot shown in Fig. 4 where the gradients are proportional to the activation energy for crystallization. Values of activation energy extracted from Fig. 4 are also shown in Fig. 3, and indicate that the mechanism of crystallization changes within the amorphous range.

The crystallization onset temperatures for Ti–Si are shown in Fig. 5 together with the associated phase diagram. In the small range examined Ti–Si behaves like W–Si.

The crystallization products of both W–Si and Ti–Si alloys on a variety of substrates are given in Table I. As a general rule the primarily crystallizing phases are metastable with the equilibrium phases appearing at higher temperatures. The phase denoted "?" denotes an unidentified phase which corresponds to no known phase in the W–Si system, including the tentatively identified cubic W_3Si [15] phase. One notable feature of Table I is the appearance of the hexagonal form of WSi_2 [16] as the first phase to

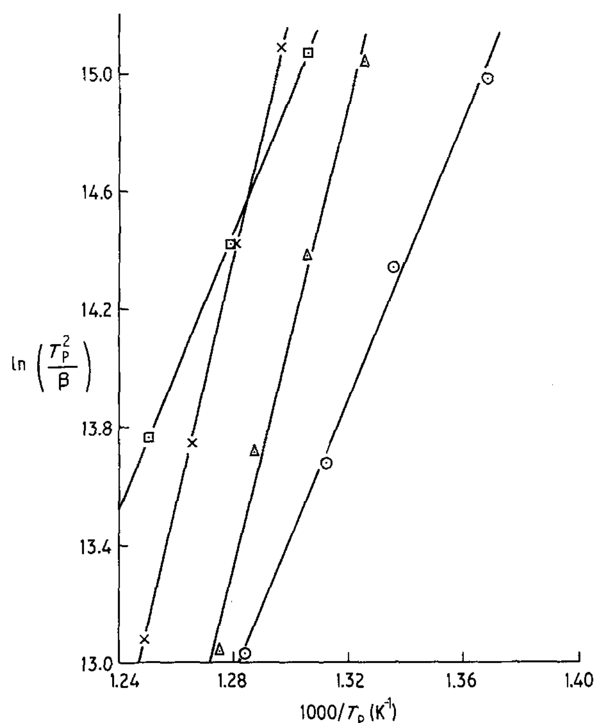

Figure 4 Kissinger plot (T_p = crystallization peak temperature, β = heating rate) for four amorphous W–Si alloys. ⊡, $W_{12}Si_{88}$; ×, $W_{45}Si_{55}$; ◬, $W_{54}Si_{46}$; ⊙, $W_{66}Si_{34}$.

crystallize across most of the range; 33 to 80 at % tungsten.

4. Discussion

4.1. Glass formation

Since most of the data relating to the formation of amorphous alloys have been derived from liquid quenched material, it is of both practical and theoretical interest to compare alloys deposited from the vapour phase with their liquid quenched counterparts. Unfortunately, in the case of the W–Ti–Si system and its associated binaries, little information appears to exist with the exception of the Ti–Si binary. Splat quenched Ti–Si alloys have been found to be amorphous only in the range 15 to 20 at % [17]. Perhaps the fastest cooling rates achieved with quenching from the melt have been obtained using the laser pulse method. Transition metal–silicon alloys prepared in this way show several extensive GFRs across the system but these are largely limited to compositions outside those occupied by equilibrium compounds [18]. It therefore appears that the greatly extended GFR obtained with sputtered alloys and the suppression of crystalline metastable and equilibrium phases can be attributed to the far higher cooling rates obtainable with deposition from the vapour. The suppression of the equilibrium phases in favour of the amorphous phase has been observed previously with sputtered WSi compositions corresponding to W_5Si_3 [19] and WSi_2 [20, 21].

A considerable number of empirical rules [22] have been suggested as guides to selecting easy glass forming compositions and there are also a number of theoretical models available [1, 17, 23, 24]. However, with the exception of the thermodynamic approach of Saunders *et al.* [25, 26] these are for liquid quenched alloys and, for the most part, do not appear applicable to this case. For example, the positions and depths of eutectics in the binary systems, and of eutectic troughs in the ternary W–Ti–Si diagram [27], do not appear to be associated with the GFR. Similarly, though the existence of very complex intermetallics is predicted to increase the likelihood of glass formation [22], all the equilibrium and metastable phases in this system have relatively simple crystal structures. One of the general rules that does apply, however, is that amorphous phase formation is difficult in areas of the phase diagram where solid solutions exist. Thus the only compositions in the W–Si (Fig. 3) and Ti–Si (Fig. 5) systems which are not amorphous on deposition correspond to terminal solid solutions in the respective phase diagrams, while Ti–W, the phase diagram of which shows complete solid solubility, is crystalline across the entire range of composition (Fig. 1). The cause of this is probably kinetic. In the as-deposited intimate mixture of elements, little diffusion is required to assume the configuration of a solid solution.

From Fig. 1 it appears that ~10 at % Si stabilizes the amorphous state in Ti–W. In this respect it is interesting to note that previous work at this laboratory

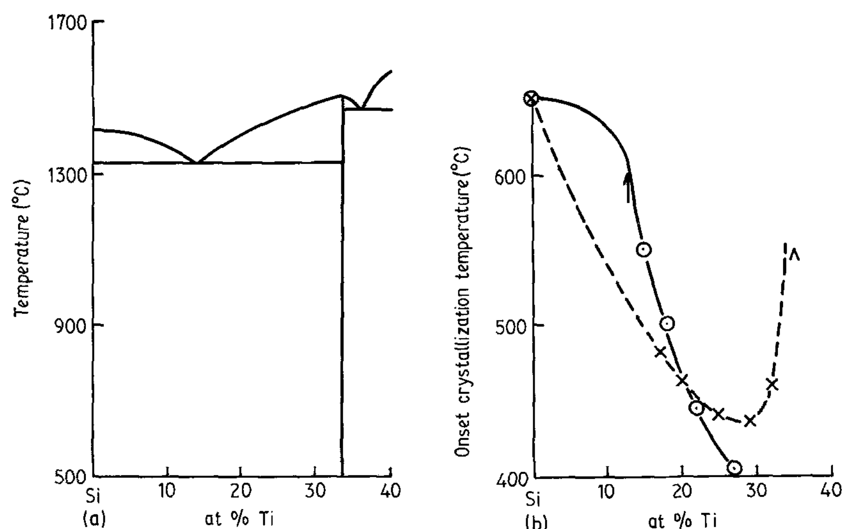

Figure 5 (a) Equilibrium diagram for Ti–Si. (b) Onset crystallization temperatures for amorphous Ti–Si alloys. ⊙, no substrate, 40° C min^{-1}, DSC. ×, Al foil substrate, 40° C min^{-1}, DSC.

TABLE I Crystallization products

Composition (at %)	Heat treatment	Substrate	Phases
33 W–67 Si	50 to 600° C/12° C min^{-1}/vacuo	Glass	Amorphous
33 W–67 Si	50 to 625° C/12° C min^{-1}/vacuo	Glass	Hexagonal WSi_2
33 W–67 Si	50 to 650° C/12° C min^{-1}/vacuo	Glass	Hexagonal WSi_2
45 to 49 W–55 to 51 Si	500° C/30 min/N_2	Si	Tetragonal WSi_2
45 to 49 W–55 to 51 Si	700° C/30 min/N_2	Si	Tetragonal WSi_2+ hexagonal WSi_2
45 to 49 W–55 to 51 Si	900° C/30 min/N_2	Si	Tetragonal WSi_2
45 to 49 W–55 to 51 Si	900° C/> 30 min/N_2	SiO_2	Tetragonal WSi_2
49 W–51 Si	50 to 550° C/40° C min^{-1}/Ar	Al	Tetragonal WSi_2
54 W–46 Si	50 to 420° C/40° C min^{-1}/Ar	None	Amorphous
54 W–46 Si	50 to 550° C/40° C min^{-1}/Ar	None	Hexagonal WSi_{2+}?
54 W–46 Si	50 to 550° C/40° C min^{-1}/Ar	Al	Hexagonal WSi_{2+}?
60 to 66 W–40 to 34 Si	500° C/30 min/N_2	Si	Hexagonal WSi_2
60 to 66 W–40 to 34 Si	700° C/30 min/N_2	Si	Hexagonal WSi_2+ tetragonal WSi_2
60 to 66 W–40 to 34 Si	900° C/30 min/N_2	Si	Tetragonal WSi_2
60 to 66 W–40 to 34 Si	900° C/> 30 min/N_2	SiO_2	Tetragonal WSi_2
76 to 80 W–24 to 20 Si	500° C/30 min/N_2	Si	Amorphous
76 to 80 W–24 to 20 Si	700° C/30 min/N_2	Si	W_5Si_{3+}?
76 to 80 W–24 to 20 Si	900° C/> 30 min/N_2	SiO_2	WO_{3+}?
80 W–20 Si	50 to 625° C/12° C min^{-1}/vacuo	Glass	Hexagonal WSi_2
80 W–20 Si	50 to 650° C/12° C min^{-1}/vacuo	Glass	Hexagonal WSi_2
22 Ti–78 Si	50 to 550° C/40° C min^{-1}/Ar	None	*c*-centred orthorhombic $TiSi_2$

suggests that oxygen is a more effective stabilizer of the amorphous phase since sputtered Ti–W alloys containing ≤ 10 at % O_2 have been found to be amorphous.

4.2. Glass stability

The correspondence between the crystallization temperatures of W–Si alloys on four different substrates and of separate films, together with the lack of substrate reaction products, suggests that some confidence can be placed in the plot of crystallization temperatures shown in Fig. 3. Three peaks are observed in the T_x curve. That around amorphous silicon is well known, while the peak at 10 to 30 at % W has been reported previously [28, 29]. The peak around the WSi_2 composition can be compared with the results of Murarka *et al.* [21] which indicated that 30 min heat treatments of amorphous $W_{31}Si_{69}$ produced hexagonal WSi_2 [16] between 300 and 400° C, which began to convert to tetragonal WSi_2 between 500 and 600° C. Our results indicate that crystallization occurs between 600 and 625° C and that the hexagonal form is stable to at least 650° C for the WSi_2 composition. However, there are large differences between the two sets of heat treatment conditions, and it is also evident from Fig. 3 that small variations in composition will produce large variations in crystallization behaviour. This could account for the differences between the two sets of results.

If the crystallization temperatures across the W–Si system are compared with the liquidus temperature, i.e. if the reduced crystallization temperatures are considered, it is seen (Fig. 3d) that a distinct peak still occurs at or near the WSi_2 composition, but that the peak corresponding to the 10 to 30 at % Si compositions is much lower. Thus the relative stability of glasses near the WSi_2 composition is much higher than any other alloy in the system (the range 80 to 100 at % Si is not included since this represents the transition to covalent bonding). It is well established that the value of the reduced crystallization temperature for metallic glasses can be as high as ~0.6, and therefore in these terms the most stable glass in the W–Si system has only moderate stability.

The thermal stability of metallic glasses has been variously associated with [30] the fastest mode of crystallization available in a particular alloy, the driving force, the kind and number of quenched-in nuclei, the time lag for homogeneous nucleation and the activation energy for diffusion. Interpretation of Figs 3 and 5 is, therefore, difficult since the crystallization temperatures give an integrated view of the influence of all the above parameters and they will all vary with composition. For example, from Table I, the mode of crystallization might be expected to be polymorphous about the WSi_2 composition, to change to primary crystallization and subsequently eutectic crystallization as the tungsten concentration increases across the W_5Si_3–WSi_2 eutectic range, and finally to become primary crystallization in the W–W_5Si_3 peritectic range. However, the above assumes that initial crystallization can be related to the equilibrium phase diagram, whereas Table I illustrates the remarkable observation that the metastable hexagonal WSi_2 phase is the first phase to form across almost the entire range of compositions. Discussion of the mode of crystallization should, therefore, more properly be associated with the (unavailable) metastable phase diagram. Equally, since the unknown free energies of the amorphous and hexagonal WSi_2 phases will vary greatly with alloy compositon, there will be large variations in the driving force for crystallization. In

fact the only parameter on which some information is available is the activation energy of crystallization which relates to the activation energy for diffusion. From Fig. 3 it is evident that, in the W–Si system, the activation energy is low about the troughs in T_x but may increase towards a peak about the WSi_2 composition. Either the diffusion mechanism or the moving species therefore changes across this range, and the increased activation energy for diffusion will contribute to the thermal stability of glasses having compositions about WSi_2.

Comparisons of Figs 3 and 5 shows that, at the Si-rich end of the binary W–Si and Ti–Si systems, T_x behaves similarly in that T_x reaches a peak about the disilicide compositions. Extrapolation of the results for amorphous alloys having compositions corresponding to WSi_2 and $TiSi_2$ into the ternary system would suggest that a tie line between these might represent a range of thermally stable alloys. The little information we have, however, shows the reverse is true (Fig. 1) though there is the added complication that a ternary phase exists in this range [27].

Enhanced thermal stability of amorphous alloys with compositions corresponding to a particular equilibrium phase has been reported previously. For example, in melt quenched Pd–Si alloys [18] compositions corresponding to equilibrium phases are all crystalline as-quenched with the exception of those about Pd_3Si. Glasses formed at and around the Pd_3Si composition were observed to have the highest crystallization temperatures in the system. However, apart from suggestions [31, 32] that factors such as the density of states at the Fermi level can determine the selective stability of particular amorphous compositions corresponding to equilibrium, low co-ordination, intermetallic phases, the reason for the high relative stability of the WSi_2 composition observed in the present work is unclear.

5. Conclusions

1. Any sputtered alloy in the W–Ti–Si system is amorphous unless the silicon level falls below 10 at % Si.

2. The amorphous range in the binary W–Si and Ti–Si systems is limited only by the presence of terminal solid solutions in the respective phase diagrams.

3. Sputtered Ti–W alloys are crystalline throughout the complete range of composition.

4. The most stable amorphous alloys in the W–Si system exist in the range 10 to 30 at % Si and 60 to 70 at % Si and amorphous diffusion barrier layers should have compositions within this range.

References

1. S. TAKAYAMA, *J. Mater. Sci.* **11** (1976) 164.
2. R. WANG, *Bull. Alloy Phase Diagrams* **2** (1981) 269.
3. S. P. MURARKA, *J. Vac. Sci. Tech.* **17** (1980) 775.
4. K. SUYAMA, H. SHIMIZU, S. YOKAGAWA, U. NAKAYAMA and A. SHIBATOMI, *Jpn. J. Appl. Phys.* **22** (1983) 341, Suppl. 22–1.
5. K. N. TU, *ibid.* **22** (1983) 147.
6. T. YAMAGUCHI, S. MORIMOTO, H. K. PARK and G. C. EIDEN, *IEEE Trans. Electron Devices* **ED-32** (1985) 184.
7. R. S. NOWICKI and M.-A. NICOLET, *Thin Solid Films* **96** (1982) 317.
8. D. PRAMANIK and A. N. SAXENA, *Solid State Tech.* **26** March (1983) 131.
9. M.-A. NICOLET, I. SUMI and M. FINETTI, *Solid State Tech.* **26** Dec (1983) 786.
10. A. CRHISTOU, W. T. ANDERSON Jr., M. L. BARK and J. E. DAVEY, in Proceedings of the 20th Annual Reliability Symposium IEEE (1982) p. 188.
11. A. G. TODD, P. G. HARRIS, I. H. SCOBEY and M. J. KELLY, *Solid State Electronics* **27** (1984) 507.
12. J. K. HOWARD, J. F. WHITE and P. S. HO, *J. Appl. Phys.* **49** (1978) 4083.
13. H. E. KISSINGER, *Anal. Chem.* **29** (1957) 1702.
14. T. OZAWA, *J. Thermal Analysis* **2** (1970) 301.
15. W. OBROWSKI, *J. Inst. Metals* **89** (1960) 79.
16. F. M. d'HEURLE, C. S. PETERSSON and M. Y. TSAI, *J. Appl. Phys.* **51** (1980) 5976.
17. S. H. WHANG, *Scripta Met.* **18** (1984) 309.
18. M. VON ALLMEN, E. HUBER, A. BLATTER and K. AFFOLTER, *Int. J. Rapid Solidification* **1** (1984–5) 15.
19. T. OHNISHI, N. YOKOYAMA, H. ONODERA, S. SUZUKI and A. SHIBATOMI, *Appl. Phys. Lett.* **43** (1983) 600.
20. F. MOHAMMADI and K. C. SARASWAT, *J. Electrochem. Soc.* **127** (1980) 450.
21. S. P. MURARKA, M. H. READ and C. C. CHANG, *J. Appl. Phys.* **52** (1981) 7450.
22. R. WANG, "Theory of Alloy Phase Formation", edited by L. Bennett (Met. Soc. AIME, 1980) pp. 472–5.
23. S. WHANG, *J. Non-Crystalline Solids* **61/62** (1984) 841.
24. S. H. WHANG, *Mat. Sci. Eng.* **57** (1983) 87.
25. N. SAUNDERS, A. P. MIODOWNIK and L. E. TANNER, in "Rapidly Quenched Metals", edited by S. Steeb and H. Warlimont, (Elsevier, Amsterdam, 1985), pp. 191–4.
26. N. SAUNDERS and A. P. MIODOWNIK, *CALPHAD* **9** (1985) 283.
27. V. A. MAKSIMOV and F. I. SHAMRAI, *Izv. Akad. Nauk. USSR, Metal.* (1970) 197.
28. N. A. PAPANICOLAOU, W. T. ANDERSON Jnr. and A. CHRISTOU, *Inst. Phys. Conf. Ser.* **65** (5) (1982) 407.
29. D. WILEY, H. PEREPEZKO and J. E. NORDMAN, 1980 Sandia Report, SAND 80–71, p. 67.
30. U. KOSTLER and U. HEROLD, in "Topics in Applied Physics", Vol. 46 "Glassy Metals 1", Ch. 10, edited by H. J. Guntherodt and H. Beck (Springer-Verlag, Berlin, Heidlberg, New York, 1981).
31. V. L. MORUZZI, P. OELHAFEN and A. R. WILLIAMS, *Phys. Rev. B* **27** (1983) 7194.
32. S. R. NAGEL and J. TAUC, *Phys. Rev. Lett.* **35** (1975) 380.

Received 29 November 1985
and accepted 21 January 1986